
ELSEVIER
CHEMICAL
ENGINEERING
JOURNAL

Chemical Engineering Journal 226 (2013) 131–138

Contents lists available at SciVerse ScienceDirect

Chemical Engineering Journal

journal homepage: www.elsevier.com/locate/cej

Photoreduction of Cr(VI) from acidic aqueous solution using TiO_2-impregnated glutaraldehyde-crosslinked alginate beads and the effects of Fe(III) ions

Yun-guo Liu *, Xin-jiang Hu, Hui Wang, An-wei Chen, Si-mian Liu, Yi-ming Guo, Yuan He, Xi Hu, Jiang Li, Shao-heng Liu, Ya-qin Wang, Lu Zhou

College of Environmental Science and Engineering, Hunan University, Changsha 410082, PR China
Key Laboratory of Environmental Biology and Pollution Control (Hunan University), Ministry of Education, Changsha 410082, PR China

HIGHLIGHTS

- Novel composites named TIGCAB were successfully prepared.
- TIGCAB are excellent photocatalysts for the reduction of Cr(VI).
- TIGCAB can be separated from reaction medium easily.
- Fe(III) ions can inhibit electron–hole recombination and promote the photoreduction of Cr(VI).
- TIGCAB can be reused for at least three cycles in batch experiments.

ARTICLE INFO

Article history:
Received 14 November 2012
Received in revised form 10 April 2013
Accepted 13 April 2013
Available online 21 April 2013

Keywords:
Cr(VI)
Acidic aqueous solution
Photoreduction
TiO_2-impregnated glutaraldehyde-crosslinked alginate beads
Fe(III)

ABSTRACT

To overcome the limitation of powder TiO_2, the TiO_2-impregnated glutaraldehyde-crosslinked alginate beads (TIGCAB) were prepared. The TIGCAB were characterized by DC, DBM, SEM, BET, XRD, Raman and TG. These synthesized beads were applied to reduce toxic Cr(VI) to Cr(III) in acidic aqueous solution under UV irradiation. In the system without TIGCAB or UV light, no chromium reduction was observed. The reduction rate of Cr(VI) was about 8% when the system was exposed to UV irradiation with blank beads. Photoreduction rate of Cr(VI) decreased with increasing pH. The reduction efficiency of Cr(VI) decreased with the increase of initial Cr(VI) concentration in the range of 5–20 mg L^{-1}. Fe(III) ions improved the photoreduction of Cr(VI) because they can promote the trapping of electrons and holes. Moreover, TIGCAB can maintain full photoreduction activity for at least three cycles. The results show that TIGCAB are promising materials for the photoreduction of Cr(VI) from acidic aqueous solution in environmental pollution cleanup.

1. Introduction

Every year, many industrial processes such as electroplating, leather tanning, and corrosion protection generate large quantities of wastewater containing various concentrations of chromium [1]. Chromium exists in natural and anthropogenically modified waters in two common oxidation states, Cr(VI) and Cr(III) [2]. Cr(VI) is very toxic to most organisms and has been classified as carcinogenic and mutagenic, whereas Cr(III) is less toxic and readily precipitates as $Cr(OH)_3$ or as the solid solution $Fe_xCr_{1-x}(OH)_3$ under alkaline or even slightly acidic conditions [2–4]. The Cr(VI) has a toxicity one hundred times higher than that of Cr(III) [5]. Reduction of Cr(VI) to Cr(III) thus leads to drastic decrease in the bioavailability and toxicity of this element, and it has become a key procedure for treating Cr(VI)-containing wastewater [6,7].

Conventional chemical reduction methods of treating Cr(VI) in water involve reduction of hexavalent chromium to the trivalent state with the use of reducing agents such as sodium thiosulfate, ferrous sulfate, sulfur dioxide gas and sodium bisulfite/metabisulfite, followed by precipitation of the insoluble Cr(III) hydroxide at neutral pH [2]. In general, with these methods large quantities of chemicals and expensive systems are required [2,8]. Compared with the conventional chemical reduction methods, the photocatalytic reduction of aqueous Cr(VI) has some obvious advantages, such as simple operation, ambient conditions, low cost, high efficiency, reusability, direct use of infinite, clean and safe natural solar energy, and no use and no release of other unwanted chemicals [9]. Titanium dioxide (TiO_2)

---

* Corresponding author at: College of Environmental Science and Engineering, Hunan University, Changsha 410082, PR China. Tel.: +86 731 88649208; fax: +86 731 88822829.
E-mail address: hnuese@126.com (Y.-g. Liu).

1385-8947/$ - see front matter © 2013 Elsevier B.V. All rights reserved.
http://dx.doi.org/10.1016/j.cej.2013.04.048

is an effective catalyst and is often used for the photocatalysis process owing to its optical and electronic properties, chemical stability and nontoxicity for the environment [10]. However, the use of TiO_2 nanopowder is limited to simple applications because significant post-treatment filtration is required to remove the TiO_2 from the final solution [11]. Therefore, many researchers undertook many attempts to entrap TiO_2 particles in some supports for degradation of dyes and adsorption of heavy metal ions, such as entrapping TiO_2 in chitosan [11,12], activated carbon [13] and SiO_2 [14]. Those materials could provide considerable advantages: minimal clogging in continuous flow systems, easier solid–liquid separation and ease of regeneration and reuse of the TiO_2.

Alginate, extracted mainly from brown seaweeds and bacteria, is a water soluble linear polysaccharide composed of β-D-mannuronic and α-L-guluronic acid residues arranged in a nonregular, and blockwise fashion along the chain [15,16]. In the presence of divalent cations such as Ca^{2+}, Cu^{2+} and Ba^{2+}, alginate can form stable hydrogels with the formation of a three-dimensional network [17]. Based on this property, alginate is widely used for the immobilization of various materials, such as algal biomass, microorganisms and enzymes [17]. Alginate is considered as promising support for photocatalysts and has been continuously studied in recent years. However, as the divalent cations are removed by a chelating agent or by a high concentration of ions such as Na^+ or Mg^{2+} [18], the crosslinking in the gel decreases and the gels are destabilized. This can lead to leakage of entrapped material and solubilization of the alginate polymers [19]. To overcome such problems, some cross-linking agents such as glutaraldehyde and epichlorohydrin are used to ensure the beads have good mechanical performance and stable chemical properties, and the glutaraldehyde is the most widely used. The crosslinking reaction took place between the aldehyde groups of glutaraldehyde and the hydroxyl groups of alginate polymers [20].

Fe(III) ions are extensively present in both natural environment and industrial effluents [21]. Fe(III) and Cr(VI) ions are often used together in many industrial processes such as mining, iron-steel, metal cleaning, plating, metal processing, automobile parts manufacture and dyeing [22]. Therefore, there is a high possibility that Cr(VI) and Fe(III) could exist together in mixed contaminant systems and the existence of Fe(III) ions tend to influence the photoreduction of Cr(VI). The application of TiO_2-impregnated glutaraldehyde-crosslinked alginate beads (TIGCAB) as photocatalysts in the reduction of Cr(VI) ions from acidic aqueous solution is still scarce, especially in the presence of Fe(III) ions. It is therefore important to study the reduction behaviors of Cr(VI) ions in the presence of Fe(III) ions.

In the present paper, TiO_2-impregnated glutaraldehyde-cross-linked alginate beads (TIGCAB) were prepared. TiO_2 photocatalysts were effectively dispersed and impregnated into the calcium alginate beads. The beads were cross-linked with glutaraldehyde to avoid the leakage of TiO_2. The TIGCAB were characterized using DC, DBM, SEM, BET, XRD, Raman and TG. Photocatalytic property was investigated based on Cr(VI) as the reduction substance. Background experiments were conducted. The effects of the process parameters such as pH, initial Cr(VI) concentration and Fe(III) ions on Cr(VI) reduction were investigated. The possible Cr(VI) photoreduction mechanism as well as the reusability of the TIGCAB were investigated in detail.

2. Materials and methods

2.1. Chemicals

Sodium alginate (SA) and TiO_2 were provided by Sinopharm Chemical Reagent Co., Ltd. The main physical and chemical characteristics of the TiO_2 are shown in Table 1. Glutaraldehyde was purchased from Tianjin Guangfu Fine Chemical Research Institute. Stock solution (1 g L^{-1}) of Cr(VI) was prepared by dissolving 2.829 g $K_2Cr_2O_7$ in 1000 mL ultrapure water. The solutions of different concentrations used in various experiments were obtained by dilution of the stock solution. The pH value of the solution in present study was adjusted to the required values by adding negligible amounts of 0.1 M NaOH or HCl solutions.

2.2. Synthesis and characterization of TIGCAB

The TIGCAB were prepared by entrapping TiO_2 nanoparticles in the calcium alginate beads. About 100 mL of the precursor solution was prepared by mixing 1.5 g of sodium alginate powder and 1.5 g of TiO_2 powder in ultrapure water and stirring until a homogenous solution was achieved. The mixture (100 mL) was injected dropwise into 400 mL $CaCl_2$ solution (4%) using a syringe (10 mL) with a needle (0.5 mm in diameter, 20 mm in length) to form TiO_2-impregnated alginate beads (TIAB). The TIAB were cured in the $CaCl_2$ (4%) solution for 4 h at room temperature and then rinsed with ultrapure water for several times. Then, the TIAB were cross-linked with 200 mL glutaraldehyde (1%) and HCl (0.1 M) solution at 40 °C under magnetic stirring (120 rpm) for 4 h [23,24]. After the cross-linking period, the beads were washed several times with ultrapure water and kept in 4% $CaCl_2$ solution and stored at room temperature for use. The preparation process is presented in Fig. 1. Blank beads were prepared by the same method without TiO_2 addition.

The size and morphology of the TIGCAB were determined by digital camera (DC, Canon IXUS130), digital biological microscope (DBM, Boyu DMS-655P) and scanning electron microscope (SEM, Hitachi TM 3000). The size of the TiO_2 powder was obtained by Zeta Sizer and Nano series equipped with a microprocessor unit (Malvern ZEN3690). The BET specific surface areas of the TiO_2 and TIGCAB were determined by the N_2 adsorption–desorption method (Beckman Coulter SA 3100). The structure of TIGCAB was determined by an X-ray diffractometer (XRD, Rigaku D/max-2500). Quantitative analysis of the phases in the TiO_2 was carried out via the Rietveld refinement method employing XRD Analysis Software (Jade 9.0). The Raman spectra were carried out using a Raman spectrometer (JY Labram-010). TG curves of TiO_2, TIGCAB and blank beads were recorded using thermoanalytical equipment (NETZSCH STA 449C) under air from room temperature to 800 °C at a heating rate of 10 °C min^{-1}.

2.3. Photocatalytic experiments

Photocatalytic experiments were conducted in a beaker in the center of which was placed a quartz tube (25 mm in diameter, 140 mm long) housing an 8 W UV-lamp (Nanke, 365 nm, 18 mm in diameter, 100 mm long). For all photocatalytic runs, 10 g (wet weight) of TIGCAB were introduced into 1000 mL of Cr(VI) solution, and the reactor contents were magnetically stirred. All experiments were performed at 25 °C in presence of air in a thermostat

Table 1
Physical and chemical characteristics of TiO_2 used in the study.

Titanium dioxide content[a]	⩾98%
Appearance[a]	White powder
Loss of weight on ignition[a]	⩽1.0%
Mean diameter[b]	35.5 nm
Crystal structure[b]	80.2 ± 0.2% anatasen, 19.8 ± 0.1% rutile
BET surface area[b]	48.6 m^2 g^{-1}

[a] Reported by the manufacturer.
[b] Obtained from this study.

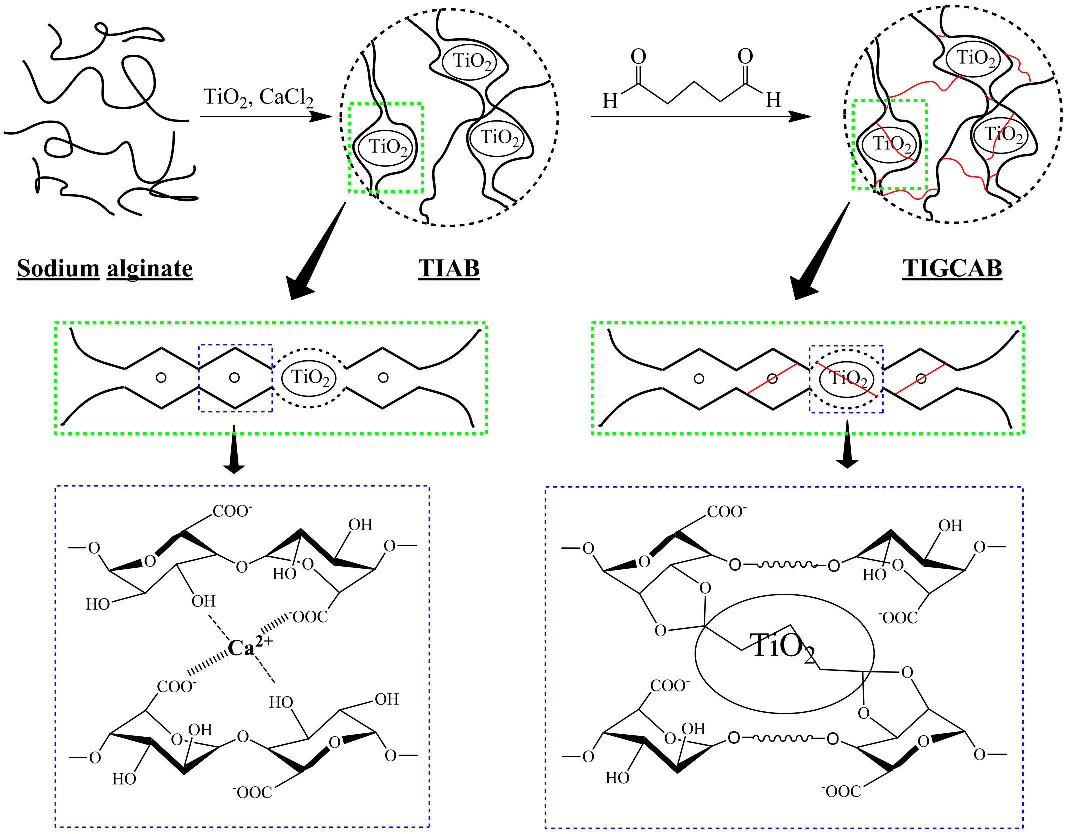

Fig. 1. Scheme for the preparation of TIGCAB.

incubator. Samples were taken periodically from the mixture and analyzed for the residual Cr(VI) concentration. The concentrations of Cr(VI) solution were determined using an UV spectrophotometer at a wavelength of 540 nm. The control experiments were conducted under three other different conditions: (i) under UV light in absence of TIGCAB; (ii) with blank beads under UV light irradiation and (iii) with TIGCAB in dark.

3. Results and discussion

3.1. Characterization of TIGCAB

Digital photo and DBM image of the TIGCAB are shown in Fig. 2. They reveal that the beads are of spherical shape with relatively uniform size of about 1.5 mm. SEM images of the beads are shown in Fig. 3. SEM characterization confirms the spherical shape of the beads (Fig. 3A) and reveals that large quantities of TiO_2 particles are deposited on the TIGCAB surface (Fig. 3B). The BET surface area of the TIGCAB was measured to be 20.4 $m^2\ g^{-1}$. Fig. 4A shows XRD spectrum of TIGCAB. From the spectrum, the intensities and positions of the observed peaks are consistent with standard XRD data for the TiO_2 with both the anatase phase (JCPDS No. 71-1166) and the rutile phase (JCPDS No. 21-1276). The weight fractions of the two crystal phases in the TiO_2 of the TIGCAB were calculated from XRD patterns utilizing the Rietveld method [25] and the result indicates that the TiO_2 in the TIGCAB is composed of 79.8 ± 0.9% anatase and 20.2 ± 1.1% rutile. This agrees well with the values of the pure TiO_2 powder (80.2 ± 0.2% for anatase and 19.8 ± 0.1% for rutile). The crystalline phase of TiO_2 was further confirmed by our Raman spectral determination. Fig. 4B shows Raman spectra of pure TiO_2 and TIGCAB. For both of samples, the peaks at ca. 142, 192, 393, 513, and 637 cm^{-1} are assigned to the five Raman-active modes of anatse phase of TiO_2 with E_g, E_g, B_{1g}, A_{1g}, and E_g, respectively [26], and the weak peak located at ca. 448 cm^{-1} is assigned to the rutile phase (other peaks may be overlapped by anatase peaks). This result shows that the TiO_2 contains both anatase and rutile according to the Raman spectrum, which is well accordant with the result of XRD (Fig. 4A). The TiO_2 content in TIGCAB was determined by TG in air, and the results are shown in Fig. 4C. The pure TiO_2 only lose about 1.04% of total weight up to 800 °C under air. However, the TIGCAB lose about 49.80% of total weight, mainly ascribed to the loss of the alginate beads. Besides, the blank beads lose about 82.64% of total weight. So the proportion of the TiO_2 in TIGCAB is about 40.25%. The TG curve of TIGCAB shows significant weight loss (13.76%) between 22 and 168 °C, which is attributed to the dehydration process. TIGCAB were found to have 36.04 wt.% weight loss when the temperature range from

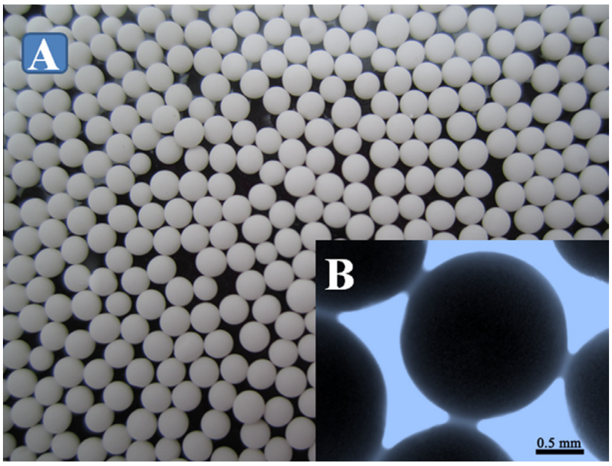

Fig. 2. The digital photo (A) and DBM image (B) of the TIGCAB.

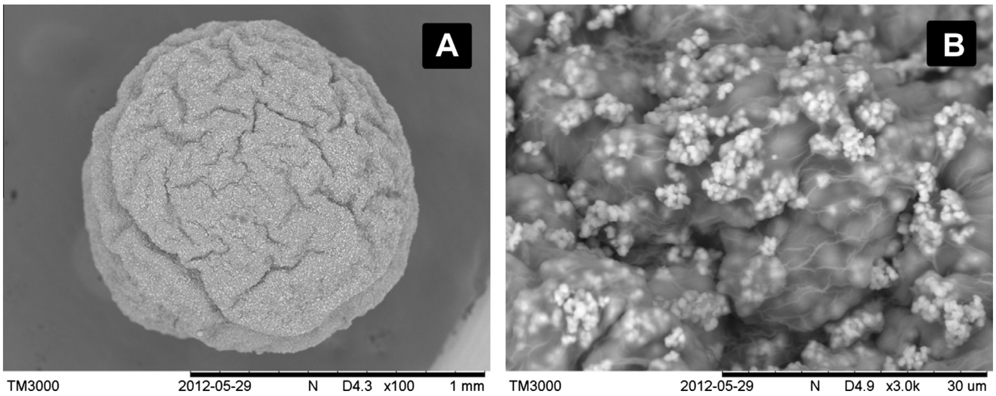

Fig. 3. The SEM characterization of TIGCAB: (A) 100× and (B) 3000×.

168 to 800 °C, which is mainly due to oxidation of the organic matters.

3.2. Background experiments

The results of background experiments are shown in Fig. 5. The first background experiment was conducted to investigate the extent of Cr(VI) reduction by UV irradiation alone. Without any TIGCAB in the reactors, a solution containing 10 mg L^{-1} of Cr(VI) was irradiated by UV light for 15 h at pH 2 at constant temperature (25 °C). As can be observed from Fig. 5, without TIGCAB, photochemical reaction of Cr(VI) under 15 h of UV light irradiation was negligible. This indicates that Cr(VI) cannot be reduced by UV irradiation in the absence of any photocatalyst. A previous study by Tsai et al. [7] also obtained a similar result. The second background experiment was conducted with blank beads under UV irradiation, and the rate of Cr(VI) reduction was about 8%. The percentage reduction of the Cr(VI) may be due to the photoreduction via the photoinduced electron transfer between the excited Cr(VI) ion and the blank beads [27].

In order to investigate the adsorption effect of Cr(VI) onto TIGCAB, the third background experiment was conducted in the presence of TIGCAB in dark. Briefly, 10 g of TIGCAB were introduced into 1000 mL of Cr(VI) solution (10 mg L^{-1}) and stirred in a dark room for 15 h at pH 2. The experimental data (Fig. 5) shows that the final concentration of Cr(VI) after 15 h of adsorption was almost equal to the initial concentration (only about 1%). The result showed that the adsorption of Cr(VI) by TIGCAB in dark was negligible. Conversely, when the system was exposed to UV light, rapid decrease in Cr(VI) concentration was observed. The results show that UV light energy is of crucial importance in Cr(VI) reduction and proposed that photocatalytic activity for the reduction of Cr(VI) ions over TiO_2 of the TIGCAB may occur through direct reduction by the photo-generated electrons [28].

3.3. Cr(VI) removal efficiency of the TIGCAB

3.3.1. Effect of pH

Solution pH is a critical variable since it directly relates to the oxidative power for the photo-generated holes as well as the reduction of Cr(VI) [29]. Fig. 6A exhibits the influence of pH (2, 3, 4, 5 and 6) on the photocatalytic process at 10 mg L^{-1} Cr(VI) concentration and 10 g L^{-1} TIGCAB at 25 °C. As seen from Fig. 6A, photoreduction was strongly dependent on the solution pH and was favored at acidic conditions. The photocatalytic efficiency is almost 100% at pH 2 after 15 h duration of irradiation, however, the efficiency decreased with increasing pH, being approximately 10% at pH 6. Similar trend was also observed with the removal of Cr(VI) using magnetic photocatalyst beads [28]. Fig. 6B shows the influence of pH (2, 3, 4, 5 and 6) on the reduction of Cr(VI) with TIGCAB and blank beads under UV, UV (without TIGCAB), TIGCAB in dark. As can be observed, with blank beads, the reduction efficiency decreased with increasing pH. In the system without TIGCAB, no appreciable photoreduction was observed at various pH values as Cr(VI) is stable and cannot yet be decomposed [28]. Cr(VI) reduction rates at various pH values were only about 1% when the system was not exposed to UV with TIGCAB.

The pH of the aqueous solution affects the speciation of chromium and the ionization state of functional groups on the TiO_2 surface. Cr(VI) exists in different forms in aqueous solution and the stability of these forms is dependent on the pH of the system. In the pH range of 1.0–6.0, different forms of chromium ions such as $Cr_2O_7^-$, $HCrO_4^-$, $Cr_3O_{10}^{2-}$, $Cr_4O_{13}^{2-}$ coexist [30]. At pH 2, the chromium ions exist predominantly in the form of $HCrO_4^-$ [31]. Besides, UV irradiation exposes more TiO_2 on the surface of the beads, and the hydroxyl groups of TiO_2 can act as efficient anchors for Cr(VI) ions [11]. The hydroxyl groups (–OH) of TiO_2 would be in protonated cationic form ($-OH_2^+$) to a higher extent in acidic solution which result in an attraction for the $HCrO_4^-$ ions in the solution. Under UV light irradiation, pairs of electron–holes are created in the TiO_2 when the energy provided (photon) is larger than or equal to the band gap (3.2 eV), as written in the following equation:

$$TiO_2 + h\nu \rightarrow TiO_2^* \ (e_{cb}^- + h_{vb}^+) \qquad (1)$$

where cb is the conduction band and vb is the valence band. Generated electron–hole pairs can either recombine and release heat energy or interact separately with other molecules. At lower pH solution, Cr(VI) anions adsorbed on the surface of the TiO_2 capture the photo-generated conduction band electrons and their reduction occurs (Eq. (2)). And water is oxidized by the photo-generated valence band holes (Eq. (3)), thus completing the redox cycle [32]. As pH increases, the interaction between chromium ions and TiO_2 becomes weaker and led to the decrease of photocatalytic reaction.

$$HCrO_4^- + 7H^+ + 3e_{cb}^- \rightarrow Cr^{3+} + 4H_2O \qquad (2)$$

$$2H_2O + 4h_{vb}^+ \rightarrow O_2 + 4H \qquad (3)$$

3.3.2. Effect of initial Cr(VI) concentration

It is important both from mechanistic and application points of view to study the dependence of the photocatalytic reaction rate on the substrate (pollutant) concentrations [33]. Hence, the effect of the initial concentration of Cr(VI) (5, 10, and 20 mg L^{-1}) on the photoreduction efficiency was studied at pH 2 and the obtained results are illustrated in Fig. 7. As shown in Fig. 7, the photoreduction

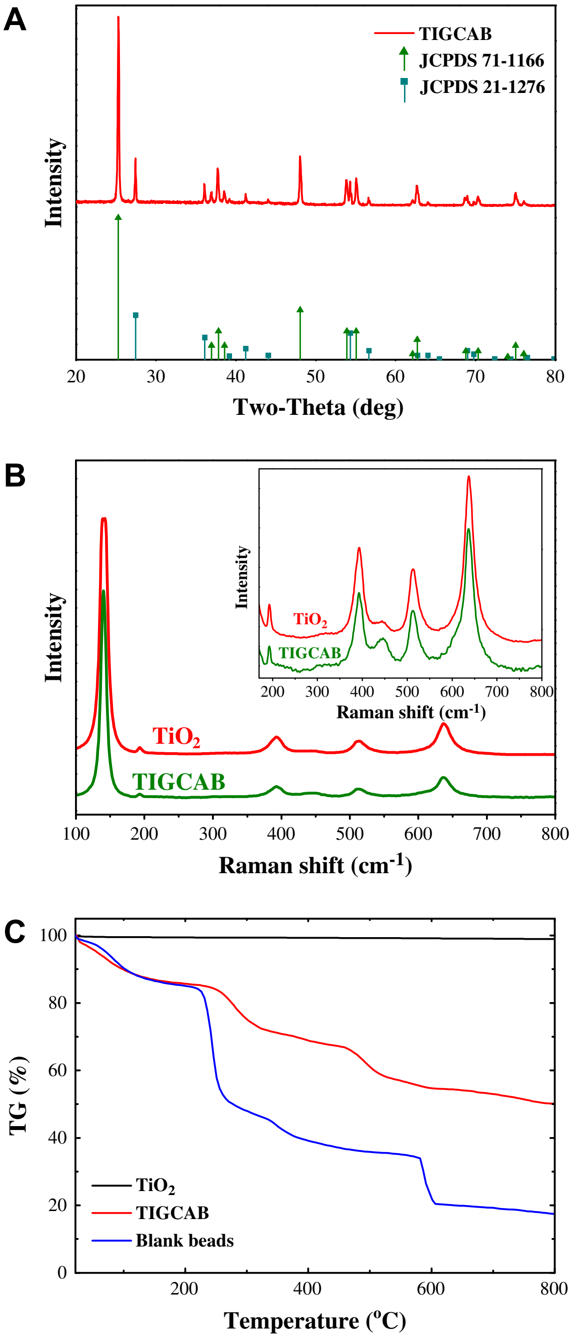

Fig. 4. (A) The XRD spectrum of TIGCAB; (B) the Raman spectra of TiO_2 and TIGCAB and (C) TG curves of TiO_2, TIGCAB and blank beads.

of Cr(VI) by TiO_2 of TIGCAB at an initial concentration of 5 mg L^{-1} reached equilibrium after 12 h, while for the initial concentrations of Cr(VI) at 10 mg L^{-1} and 20 mg L^{-1} were around 15 h and 27 h, respectively. At equilibrium, the reduction efficiencies of Cr(VI) at initial Cr(VI) concentrations of 5, 10 and 20 mg L^{-1} were 100%, 100% and 99%, respectively. The photoreduction was completed within a reaction time of 12 h when the initial Cr(VI) concentration was 5 mg L^{-1}, but only about 90% and 37% of reduction were observed at 10 mg L^{-1} and 20 mg L^{-1}, respectively. This may be due to the fact that for a fixed dosage of TIGCAB, the total available electron–hole pairs were limited to obtain a higher reduction efficiency of Cr(VI) at higher concentration [28].

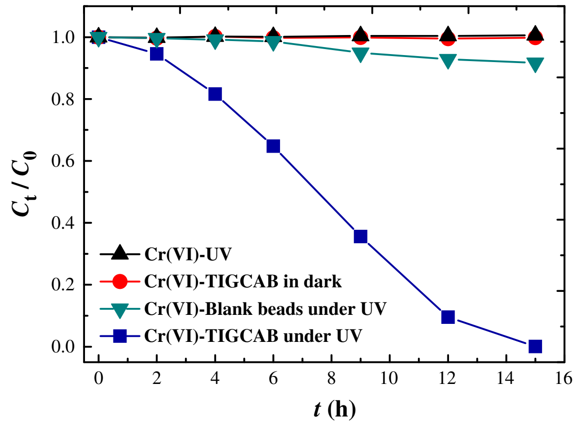

Fig. 5. Comparison of the photocatalytic performance with UV (without TIGCAB), TIGCAB in dark, blank beads and TIGCAB under UV. Conditions: initial Cr(VI) concentration, 10 mg L^{-1}; volume, 1000 mL; amount of wet TIGCAB or blank beads, 10 g L^{-1}; initial pH, 2.0; temperature, 25 °C.

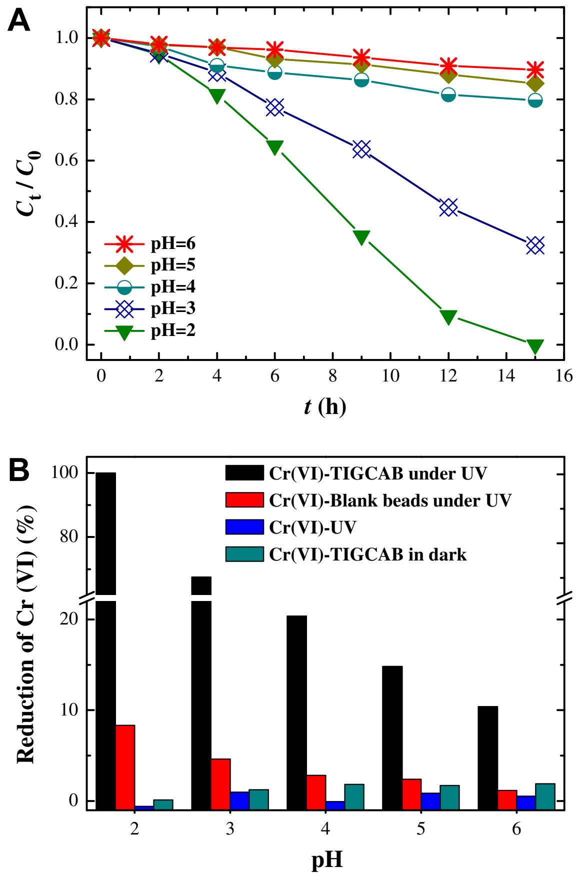

Fig. 6. (A) Influence of pH (2, 3, 4, 5 and 6) on the Cr(VI) reduction using TIGCAB and (B) comparison of the effect of initial pH (2, 3, 4, 5 and 6) on the reduction of Cr(VI) with UV (without TIGCAB), TIGCAB in dark, blank beads and TIGCAB under UV. Conditions: initial Cr(VI) concentration, 10 mg L^{-1}; volume, 1000 mL; amount of wet TIGCAB or blank beads, 10 g L^{-1}; temperature, 25 °C.

3.3.3. Effect of presence of Fe(III) ions

Fig. 8A shows the time course of photoreduction of Cr(VI) in the presence of various initial concentrations Fe(III) ions (0, 0.02, 0.05 and 0.1 mmol L^{-1}). As seen from Fig. 8A, reduction of Cr(VI) in the absence of Fe(III) ions was slow and could not be completely re-

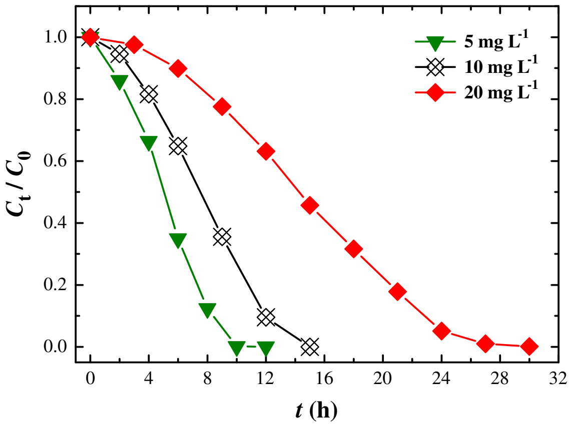

Fig. 7. Effect of initial Cr(VI) concentration (5, 10 and 20 mg L^{-1}) on the Cr(VI) photo-reduction. Conditions: volume, 1000 mL; amount of wet TIGCAB, 10 g L^{-1}; initial pH, 2.0; temperature, 25 °C.

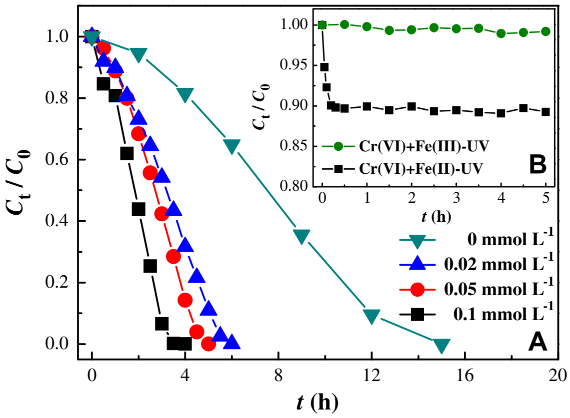

Fig. 8. (A) Effect of Fe(III) ions (0, 0.02, 0.05 and 0.1 mmol L^{-1}) on the reduction of Cr(VI). Conditions: initial Cr(VI) concentration, 10 mg L^{-1}; volume, 1000 mL; amount of wet TIGCAB, 10 g L^{-1}; initial pH, 2.0; temperature, 25 °C and (B) comparison of the effect of Fe(III) ions (0.1 mmol L^{-1}) and Fe(II) ions (0.1 mmol L^{-1}) on the Cr(VI) reduction without TIGCAB in the presence of UV. Conditions: initial Cr(VI) concentration, 10 mg L^{-1}; volume, 1000 mL; initial pH, 2.0; temperature, 25 °C.

duced until 15 h of irradiation by UV light. However, reductions of Cr(VI) were very fast and efficient, and evidently could be completely reduced within 3.5, 5, 6 h when the initial concentrations of Fe(III) ions in the system were 0.1, 0.05 and 0.02 mmol L^{-1}, respectively. The presence of Fe(III) ions had a significant promoting effect on the photoreduction of Cr(VI), which may be mainly attributed to the inhibition of electron–hole recombination and the reaction between Fe(II) and Cr(VI) [21]. When TiO_2 on the surface of the TIGCAB is irradiated with photons whose energy is equal to or greater than its band gap energy, an electron from the valence band can be excited to the conduction band, thus creating an electron–hole pair. The photo-generated electron and hole can be transferred to the adsorbed Cr(VI) ions or H_2O on the surface of the catalyst (Eqs. (2) and (3)). In competition with charge transfer to adsorbed species is electron and hole recombination [34]. If the electron–hole recombination rate is too high it can decrease the reduction efficiency of Cr(VI). In this investigation, the main form of Cr(VI) is a negatively charged Cr(VI) complex ions ($HCrO_4^-$), which is hard to capture the negative charge photo-generated electron (e_{cb}^-) due to the electrostatic repulsion. Therefore, some of the photo-generated electrons would recombine with holes which result in a slow reduction of Cr(VI) when no Fe(III) ions were present. However, when Fe(III) ions were added, the positive charge ferric ions (Fe^{3+}) could easily convert to Fe(II) ions by trapping the photo-generated electrons (Eq. (4)). And then, Cr(VI) was reduced by Fe(II) and the reduction process probably occurred via three one-electron-transfer steps (Eq. (5)), ending in Cr(III) form which is the stable final product [35]. The reductions of Cr(V) and Cr(IV) are fast and only the one-electron reduction of Cr(VI) to Cr(V) is the rate-limiting reaction due to the differences of reduction potentials between the different Cr reduction steps [36]. Therefore, the Fe(III) ions can promote the trapping of electrons and holes at the surface of TiO_2 leading to a high efficiency of photocatalysis. The proposed transfer mechanism of electrons and holes is shown in Fig. 9.

$$Fe^{3+} + e_{cb}^- \rightarrow Fe^{2+} \tag{4}$$

$$Cr(VI) \xrightarrow{Fe^{2+}} Cr(V) \xrightarrow{Fe^{2+}} Cr(VI) \xrightarrow{Fe^{2+}} Cr(III) \tag{5}$$

The overall reduction of Cr(VI) by Fe(II) at acidic condition is shown as:

$$3Fe^{2+} + HCrO_4^- + 7H^+ \rightarrow 3Fe^{3+} + Cr^{3+} + 4H_2O \tag{6}$$

Reactions (5) and (6) were confirmed in this study experimentally. The first experiment was carried out without TIGCAB at pH 2.0 with initial concentrations of 0.1 mmol L^{-1} Fe(III) and 10 mg L^{-1} Cr(VI) in the presence of UV. The experimental data (Fig. 8B) showed that the reduction rate of Cr(VI) was negligible.

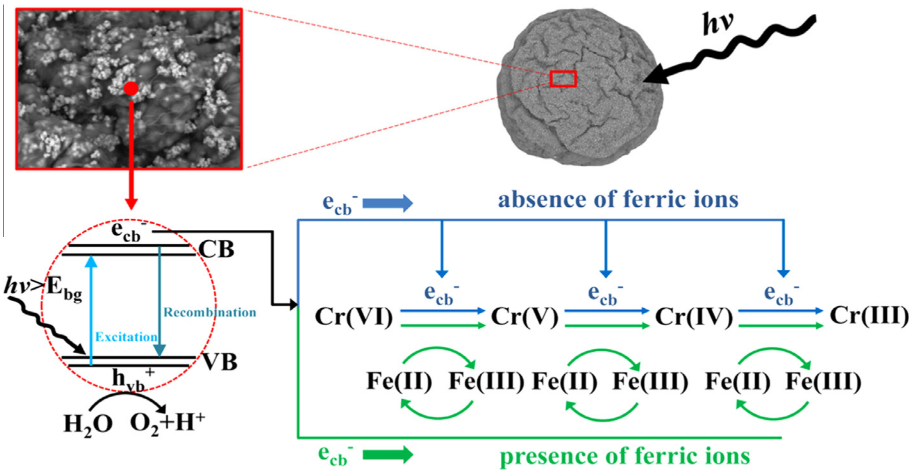

Fig. 9. The proposed photoreduction mechanism of Cr(VI) on the TIGCAB.

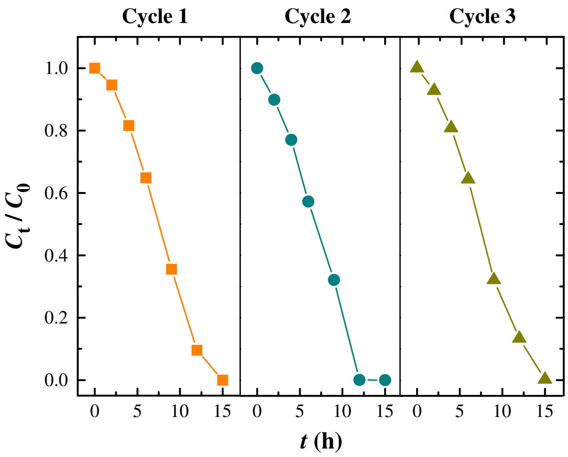

Fig. 10. Reuse of the TIGCAB. Photocatalytic conditions: initial Cr(VI) concentration, 10 mg L^{-1}; volume, 1000 mL; amount of wet TIGCAB, 10 g L^{-1}; initial pH, 2.0; temperature, 25 °C. Regeneration conditions: regeneration solution, 100 mL $CaCl_2$ (4%); contact time, 2 h; temperature, 25 °C.

In the second experiment, a solution with 0.1 mmol L^{-1} Fe(II) and 10 mg L^{-1} Cr(VI) was irradiated by UV light for 5 h at pH 2 in the absence of TIGCAB. As can be observed from Fig. 8B, the Cr(VI) concentration decreased with illumination time, which may be due to the homogeneous reaction between Cr(VI) and Fe(II).

3.4. Reuse of the TIGCAB

For practical application, the recycling of the photocatalyst is essential. In this study, at the end of each cycle (initial Cr(VI) concentration, 10 mg L^{-1}; amount of wet TIGCAB, 10 g L^{-1}; initial pH, 2.0; temperature, 25 °C), the TIGCAB were separated from the solution by filtration and then added into 100 mL $CaCl_2$ solution (4%) and stirred for 2 h at 25 °C and rinsed with ultrapure water. After regeneration, the TIGCAB were used in the following cycle. From Fig. 10, it is observed that the TIGCAB retained their activity fully after recycle for three times, indicating that they have a good reusability.

4. Conclusion

The TiO_2-impregnated glutaraldehyde-crosslinked alginate beads (TIGCAB) have been successfully synthesized and they can be applied for the photoreduction of Cr(VI) from acid aqueous solution using a photocatalytic process. The results of background experiments showed that both of TIGCAB and UV light are essential in the photoreduction process. The solution pH and initial concentration of Cr(VI) greatly influenced the photoreduction of Cr(VI). The presence of Fe(III) ions may serve as an effective electron acceptor to increase the photoreduction of Cr(VI) ions due to the inhibition of electron–hole recombination and the reaction between Fe(II) and Cr(VI). Finally, TIGCAB can be reused without losing effectiveness for at least three cycles in batch experiments.

Acknowledgements

The authors would like to thank financial support from the National Natural Science Foundation of China (Grant No. 41271332), the Natural Science Foundation of Hunan province, China (Grant No. 11JJ2031) and the Hunan Provincial Innovation Foundation For Postgraduate (Grant No. CX2012B138).

References

[1] D. Blowes, Tracking hexa valent Cr in groundwater, Science 295 (2002) 2024–2025.
[2] J.T. Juan, A.G. María, I.L. Marta, Heterogeneous photocatalytic reduction of Chromium(VI) over TiO_2 particles in the presence of oxalate: involvement of Cr(V) species, Environ. Sci. Technol. 38 (2004) 1589–1594.
[3] J. Kotaś, Z. Stasicka, Chromium occurrence in the environment and methods of its speciation, Environ. Pollut. 107 (2000) 263–283.
[4] D. Rai, B.M. Sass, D.A. Moore, Chromium(III) hydrolysis constants and solubility of Chromium(III) hydroxide, Inorg. Chem. 26 (1987) 345–349.
[5] G.C.C. Yang, S.W. Chan, Photocatalytic reduction of chromium(VI) in aqueous solution using dye-sensitized nanoscale ZnO under visible light irradiation, J. Nanopart. Res. 11 (2009) 221–230.
[6] P. Mytych, A. Karocki, Z. Stasicka, Mechanism of photochemical reduction of chromium(VI) by alcohols and its environmental aspects, J. Photochem. Photobiol. A 160 (2003) 163–170.
[7] Y.P. Tsai, R.A. Doong, J.C. Yang, Y.J. Wu, Photo-reduction and adsorption in aqueous Cr(VI) solution by titanium dioxide, carbon nanotubes and their composite, J. Chem. Technol. Biotechnol. 86 (2011) 949–956.
[8] N. Daneshvar, D. Salari, S. Aber, Chromium adsorption and Cr(VI) reduction to trivalent chromium in aqueous solutions by soya cake, J. Hazard. Mater. B 94 (2002) 49–61.
[9] Y.C. Zhang, J. Li, M. Zhang, D.D. Dionysiou, Size-tunable hydrothermal synthesis of sns_2 nanocrystals with high performance in visible light-driven photocatalytic reduction of aqueous Cr(VI), Environ. Sci. Technol. 45 (2011) 9324–9331.
[10] K. Rajeshwar, J.G. Ibanez, Environmental Electrochemistry, Academic Press, San Diego, USA, 1997.
[11] S.M. Miller, J.B. Zimmerman, Novel, bio-based, photoactive arsenic sorbent: TiO_2-impregnated chitosan bead, Water Res. 44 (2010) 5722–5729.
[12] X. Zhang, X. Zhao, H. Su, Degradation characteristic of TiO_2-chitosan adsorbent on Rhodamine band purification of industrial wastewater, Korean J. Chem. Eng. 28 (2011) 1241–1246.
[13] X. Zhang, M. Zhou, L. Lei, TiO_2 photocatalyst deposition by MOCVD on activated carbon, Carbon 44 (2006) 325–333.
[14] T. Yuranova, R. Mosteco, J. Bandara, D. Laub, J. Kiwi, Self-cleaning cotton textiles surfaces modified by photoactive SiO_2/TiO_2 coating, J. Mol. Catal. A 244 (2006) 160–167.
[15] S. Peretz, O. Cinteza, Removal of some nitrophenol contaminants using alginate gel beads, Colloids Surf. A 319 (2008) 165–172.
[16] A. Martinsen, G. Skjak-Brak, O. Smidsrod, Alginate as immobilization material: I. Correlation between chemical and physical properties of alginate gel beads, Biotechnol. Bioeng. 33 (1989) 79–89.
[17] S.K. Papageorgiou, F.K. Katsaros, E.P. Favvas, G.E. Romanos, C.P. Athanasekou, K.G. Beltsios, O.I. Tzialla, P. Falaras, Alginate fibers as photocatalyst immobilizing agents applied in hybrid photocatalytic/ultrafiltration water treatment processes, Water Res. 46 (2012) 1858–1872.
[18] I.W. Sutherland, Alginates, in: D. Byrom (Ed.), Biomaterials; Novel Materials from Biological Sources, Stockton, New York, 1991, pp. 309–331.
[19] W.R. Gombotz, S.F. Wee, Protein release from alginate matrices, Adv. Drug Deliv. Rev. 31 (1998) 267–285.
[20] C.K. Yeom, K.H. Lee, Characterization of sodium alginate membrane crosslinked with glutaraldehyde in pervaporation separation, J. Appl. Polym. Sci. 67 (1998) 209–219.
[21] D. Chen, A.K. Ray, Removal of toxic metal ions from wastewater by semiconductor photocatalysis, Chem. Eng. Sci. 56 (2001) 1561–1570.
[22] Y. Sağ, Ü. Açikel, Z. Aksu, T. Kutsal, A comparative study for the simultaneous biosorption of Cr(VI) and Fe(III) on *C. vulgaris* and *R. arrhizus*: application of the competitive adsorption models, Process Biochem. 33 (1998) 273–281.
[23] A.W. Chan, R.A. Whitney, R.J. Neufeld, Semisynthesis of a controlled stimuli-responsive alginate hydrogel, Biomacromolecules 10 (2009) 609–616.
[24] J.H. Chen, Q.L. Liu, S.R. Hu, J.C. Ni, Y.S. He, Adsorption mechanism of Cu(II) ions from aqueous solution by glutaraldehyde crosslinked humic acid-immobilized sodium alginate porous membrane adsorbent, Chem. Eng. J. 173 (2011) 511–519.
[25] M. Gharagozlou, Y. Ganjkhanlou, Effect of Fe addition on phase transformation of titanium dioxide nanocrystals prepared by Pechini-type sol–gel method, Micro Nano Lett. 7 (2012) 872–875.
[26] T. Ohsaka, F. Izumi, Y.J. Fujiki, Raman spectrum of anatase, TiO_2, J. Raman Spectrosc. 7 (1978) 321–324.
[27] P. Mytych, A. Karocki, Z. Stasicka, Mechanism of photochemical reduction of chromium(VI) by alcohols and its environmental aspects, J. Photochem. Photobiol. A: Chem. 160 (2003) 163–170.
[28] A. Idris, N. Hassan, N.S.M. Ismail, E. Misran, N.M. Yusof, A. Ngomsik, A. Bee, Photocatalytic magnetic separable beads for chromium(VI) reduction, Water Res. 44 (2010) 1683–1688.
[29] H.T. Hsu, S.S. Chen, Y.S. Chen, Removal of chromium(VI) and naphthalenesulfonate from textile wastewater by photocatalysis combining ionic exchange membrane processes, Sep. Purif. Technol. 80 (2011) 663–669.
[30] S.M. Nomanbhay, K. Palanisamy, Removal of heavy metal from industrial wastewater using chitosan coated oil palm shell charcoal, Electron. J. Biotechnol. 8 (2005) 43–53.
[31] X.J. Hu, J.S. Wang, Y.G. Liu, X. Li, G.M. Zeng, Z.L. Bao, X.X. Zeng, A.W. Chen, F. Long, Adsorption of chromium (VI) by ethylenediamine-modified cross-linked

magnetic chitosan resin: isotherms, kinetics and thermodynamics, J. Hazard. Mater. 185 (2011) 306–314.

[32] T. Papadam, N.P. Xekoukoulotakis, I. Poulios, D. Mantzavinos, Photocatalytic transformation of acid orange 20 and Cr(VI) in aqueous TiO_2 suspensions, J. Photochem. Photobiol. A 186 (2007) 308–315.

[33] M. Qamar, M.A. Gondal, Z.H. Yamani, Synthesis of nanostructured NiO and its application in laser-induced photocatalytic reduction of Cr(VI) from water, J. Mol. Catal. A: Chem. 341 (2011) 83–88.

[34] A.L. Linsebigler, G. Lu, J.T. Yates, Photocatalysis on TiO_2 surfaces: principles, mechanisms, and selected results, Chem. Rev. 95 (1995) 735–758.

[35] D.L. Sedlak, P.G. Chan, Reduction of hexavalent chromium by ferrous iron, Geochim. Cosmochim. Acta 61 (1997) 2185–2192.

[36] S.J. Hug, H.U. Laubscher, B.R. James, Iron(III) catalyzed photochemical reduction of chromium(VI) by oxalate and citrate in aqueous solutions, Environ. Sci. Technol. 31 (1997) 160–170.